2015

Measurement of the EMC effect in the deuteron

K. A. Griffioen
College of William and Mary

J. Arrington

M. E. Christy

N. Kalantarians

Measurement of the EMC Effect in the Deuteron

K.A. Griffioen,[1] J. Arrington,[2] M.E. Christy,[3] R. Ent,[4] N. Kalantarians,[3] C.E. Keppel,[4] S.E. Kuhn,[5] W. Melnitchouk,[4] G. Niculescu,[6] I. Niculescu,[6] S. Tkachenko,[7] and J. Zhang[7]

[1] *College of William and Mary, Williamsburg, Virginia 23187, USA*
[2] *Argonne National Laboratory, Argonne, Illinois 60439*
[3] *Hampton University, Hampton, Virginia 23668, USA*
[4] *Thomas Jefferson National Accelerator Facility, Newport News, Virginia 23606, USA*
[5] *Old Dominion University, Norfolk, Virginia 23529, USA*
[6] *James Madison University, Harrisonburg, Virginia 22807, USA*
[7] *University of Virginia, Charlottesville, Virginia 22901, USA*

(Dated: June 29, 2015)

We have determined the structure function ratio $R^d_{\rm EMC} = F_2^d/(F_2^n + F_2^p)$ from recently published F_2^n/F_2^d data taken by the BONuS experiment using CLAS at Jefferson Lab. This ratio deviates from unity, with a slope $dR^d_{\rm EMC}/dx = -0.10 \pm 0.05$ in the range of Bjorken x from 0.35 to 0.7, for invariant mass $W > 1.4$ GeV and $Q^2 > 1$ GeV^2. The observed EMC effect for these kinematics is consistent with conventional nuclear physics models that include off-shell corrections, as well as with empirical analyses that find the EMC effect proportional to the probability of short-range nucleon-nucleon correlations.

PACS numbers: 21.45.Bc, 25.30.Fj, 24.85.+p, 13.60.Hb

I. INTRODUCTION

In the early 1980s the European Muon Collaboration (EMC) discovered that deep-inelastic scattering from atomic nuclei is not simply the incoherent sum of scattering from the constituent nucleons [1]. Their data suggested that quarks with longitudinal momentum fraction x in the range 0.35 to 0.7 were suppressed in bound nucleons, and their observations were quickly confirmed at SLAC [2, 3]. The deep-inelastic structure function $F_2^A(x)$ for a nucleus with A nucleons was compared to the equivalent quantity $F_2^d(x)$ for the deuteron, such that $R^A_{\rm EMC} = (F_2^A/A)/(F_2^d/2)$. At intermediate x, $R^A_{\rm EMC}$ is less than unity, and this deviation grows with A. Over the following three decades, subsequent dedicated measurements [4–8] confirmed the EMC effect with ever-increasing precision for a wide range of nuclei. Drell-Yan data from Fermilab [9], however, which were largely sensitive to sea quarks, showed no modifications of the anti-quark sea for $0.1 < x < 0.3$, contrary to models predicting anti-quark enhancement. Despite many theoretical papers on the EMC effect, no universally accepted explanation has emerged. For reviews, see Refs. [10–12].

The precise, new measurements from Jefferson Lab on light nuclei [8] have generated a renewed interest in understanding the EMC effect. The slopes $|dR^A_{\rm EMC}/dx|$ for $0.35 < x < 0.7$ increase with A, however, the ^{9}Be slope is anomalously large, suggesting perhaps that the EMC effect is dependent on local density and that ^{9}Be might be acting like two tightly bound α particles and a neutron. A recent analysis [13] suggests that $dR^A_{\rm EMC}/dx$ is proportional to the probability of finding short-range correlations in nuclei [14–19]. Recent work on this subject [20–25] concludes that although binding and Fermi motion effects contribute, some modification of the bound nucleon's structure appears to be required to explain the EMC effect. Whether this is caused by the nuclear mean field, short-range correlations, or both is still open to debate.

EMC ratios are usually taken with respect to the deuteron, which is the best proxy for an isoscalar nucleon (neutron plus proton), but the deuteron too may exhibit an EMC effect. Several data-driven, model-dependent attempts [7, 13, 26] have been made to determine $R^d_{\rm EMC} = F_2^d/(F_2^n + F_2^p)$, in which $F_2^{n(p)}$ is the free neutron (proton) structure function. However, the lack of knowledge about the free neutron's structure has clouded these efforts. Theoretical estimates of the deuteron EMC ratio have also been made [27–39], often with the goal of isolating F_2^n/F_2^p.

A clean measurement of $R^d_{\rm EMC}$ is greatly needed. The deuteron is weakly bound (by 2.2 MeV), and the nucleons are governed only by the *pn* interaction. Therefore, a precise measurement of $R^d_{\rm EMC}$ can shed light on the cause of the EMC effect. Because the deuteron has a weak mean field (1 MeV/nucleon binding versus 8 MeV/nucleon for heavier nuclei), but a substantial contribution from high-momentum *pn* pairs, it is a good test-case.

II. DATA ANALYSIS

A new extraction of $R^d_{\rm EMC}$ with smaller uncertainties on F_2^n is now possible thanks to the high-quality data from the BONuS experiment [40–42] using CLAS at Jefferson Lab with electron beams up to 5.26 GeV. BONuS was designed to measure the high-x structure function ratio F_2^n/F_2^p using a model-independent extraction of F_2^n that relies on the spectator tagging technique. The experiment used a 7-atmosphere gaseous deuterium target surrounded by a radial time projection chamber capable of detecting recoil protons in the range 70-200 MeV/c

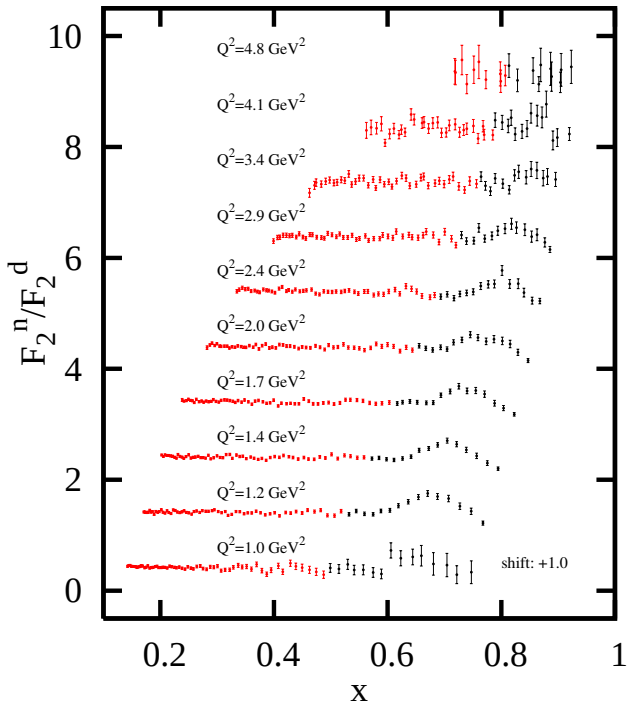

FIG. 1: (color online). BONuS data for F_2^n/F_2^d vs. Bjorken x taken with a 5.26 GeV beam. Only data for $Q^2 \geq 1$ GeV^2 are shown. The red points ($W > 1.4$ GeV) are used in this analysis. Error bars are statistical only. Each spectrum is shifted upward by 1.0 from the set below it.

[40]. By selecting backward-going and low-momentum spectators, final-state pn interactions and off-shell effects were minimized, respectively [42]. Detection of the spectator proton ensured that the electron scattered from the neutron. The initial-state kinematics of the neutron were then calculated from the spectator momentum. This technique enabled the extraction of F_2^n/F_2^d over a wide range of x for 4-momentum transfer squared Q^2 between 0.7 and 4.5 GeV^2, which covers the resonance region and part of the deep-inelastic region. For the present analysis we have used the published data from the 4.22 and 5.26 GeV beam energies with $Q^2 \geq 1$ GeV^2 and invariant final-state mass $W > 1.4$ GeV to determine $R^d_{\rm EMC}$.

The primary data from BONuS are the ratios F_2^n/F_2^d obtained from measuring tagged neutron event rates in CLAS and dividing them by the untagged deuteron rates recorded simultaneously at the same kinematics [42]. Consequently, detector acceptance and other systematic effects largely cancel, and the accuracy of this ratio is far better than that of F_2^n alone.

The overall normalization of the BONuS data, which takes into account the spectator proton detection efficiency, was initially chosen [41] to make F_2^n/F_2^p at $x = 0.3$ agree with the CTEQ-Jefferson Lab (CJ) [43] global fit for this point. There is a 3% normalization uncertainty associated with this choice. For the final BONuS results [42], which include the resonance region, the normalization minimized the χ^2 of the full data set with respect to the most recent update [44] of the Christy and Bosted (CB) fits [45, 46]. In this case, the convolution model of Ref. [25, 36] allowed for a self-consistent extraction of F_2^n from F_2^p and F_2^d and better control over the relative normalization of F_2^n and F_2^d. The new model produced no change in the 5 GeV normalization, but a 10% increase in the magnitude of the 4 GeV data.

Figure 1 shows the BONuS F_2^n/F_2^d data set taken with a 5.26 GeV beam. The red points correspond to values of the struck neutron's invariant mass W above 1.4 GeV, whereas the black points ($W < 1.4$ GeV) are excluded from this analysis to eliminate the Δ resonance.

With the new normalization, both the 5.26 and 4.22 GeV data sets yield consistent results within the statistical uncertainties. To explore the region $x > 0.45$ we pushed our analysis into the resonance region ($1.4 < W < 2.0$ GeV). Available data, albeit at slightly higher Q^2, suggest that $R^A_{\rm EMC}$ in the resonance region is similar to that in the deep-inelastic scattering region at the same x [47]. Therefore, we expect that an average over many different Q^2 values washes out any resonance structure and that duality ensures $R^d_{\rm EMC}$ at fixed x, averaged over W, approaches the deep-inelastic limit. These assumptions were tested and confirmed within statistical and systematic uncertainties by looking for a Q^2 dependence of $R^d_{\rm EMC}$ within each x-bin and by considering variations in $R^d_{\rm EMC}$ among four kinematic cases:

1. $W > 1.4$ GeV and $Q^2 > 1$ GeV^2;
2. $W > 1.8$ GeV and $Q^2 > 1$ GeV^2;
3. $W > 2.0$ GeV and $Q^2 > 1$ GeV^2; and
4. $W > 2.0$ GeV and $Q^2 > 2$ GeV^2.

The F_2^n/F_2^d data were sorted into 20-MeV-wide W bins and into logarithmic Q^2 bins (13 per decade) with edges at 0.92, 1.10, 1.31, 1.56, 1.87, 2.23, 2,66, 3.17, 3.79, 4.52, and 5.40 GeV^2.

The analysis consisted of forming the quantity

$$r(W,Q^2) = \frac{F_2^n}{F_2^d} + \frac{F_2^p}{F_2^d}, \qquad (1)$$

in which the first term is the measured BONuS ratio and the second term is the parameterization of world data [44–46]. All data falling within one of the 20 x-bins of width 0.05 were combined using

$$\langle x \rangle = \sum_i \frac{x_i}{\sigma_i^2} \Big/ \sum_i \frac{1}{\sigma_i^2}, \qquad (2)$$

$$\langle r \rangle = \sum_i \frac{r_i}{\sigma_i^2} \Big/ \sum_i \frac{1}{\sigma_i^2}, \qquad (3)$$

$$\Delta r_{\rm stat} = \sqrt{1/\sum_i \frac{1}{\sigma_i^2}}, \quad \text{and} \qquad (4)$$

$$\Delta r_{\rm sys} = \sum_i \frac{\Delta r_{{\rm sys},i}}{\sigma_i^2} \Big/ \sum_i \frac{1}{\sigma_i^2}, \qquad (5)$$

in which σ_i are the statistical uncertainties and $\Delta r_{\mathrm{sys},i}$ are the corresponding systematic uncertainties for the ith F_2^n/F_2^d datum.

The final values for R_{EMC}^d were then calculated as

$$R_{\mathrm{EMC}}^d = 1/\langle r\rangle, \quad (6)$$
$$\Delta R_{\mathrm{EMC}}^{\mathrm{stat}} = \Delta r_{\mathrm{stat}}/\langle r\rangle^2, \quad \text{and} \quad (7)$$
$$\Delta R_{\mathrm{EMC}}^{\mathrm{sys}} = \Delta r_{\mathrm{sys}}/\langle r\rangle^2. \quad (8)$$

III. UNCERTAINTIES

Several checks on our results were made. First, the analysis was performed by directly calculating $R_{\mathrm{EMC}}^d = \langle 1/r\rangle$ using the same 20 x-bins. The final answers were nearly identical to those in which inversion was the last step. The statistical spread in the ratio r in each x-bin was used to calculate a standard error. This error agreed very well with Δr_{stat}, which supports the hypothesis that variations in r within a bin are purely statistical. Systematic bias was also studied using a cut for $Q^2 > 2$ GeV^2, which in the region of comparison showed no significant deviation from the data that include lower Q^2 values.

Overall systematic uncertainties were estimated by varying the models for F_2^p/F_2^d and the kinematic cuts. The model dependence was explored using the published CB fits and two later improvements applied to kinematic Case 1 using the 5 GeV data. The kinematic-dependence was explored using kinematic Cases 1–4 for the 5 GeV data and Case 1 for the 4 GeV data. In order to separate the overall normalization uncertainty from other systematic uncertainties, we fit the EMC slope in the range $0.35 < x < 0.7$ and rescaled the data such that the linear fit intersected unity at $x = 0.31$. This value was obtained from a global analysis of the EMC effect in all nuclei [13]. The scaling factors ranged from 0.99 to 1.01 for the different cases. The average variation in $R_{\mathrm{EMC}}^d(x)$ at fixed x for the different cases, the 1% scale uncertainty, and the BONuS systematic uncertainty $\Delta R_{\mathrm{EMC}}^{\mathrm{sys}}$ were added in quadrature to yield $\Delta R_{\mathrm{tot}}^{\mathrm{sys}}$, which is listed in Table I and shown as the blue band in Figure 2. The systematic uncertainties of the BONuS data themselves dominate at large x, whereas the model uncertainties of the global fits dominate at low x (high W). The mid-x region is dominated by the normalization uncertainty. For Case 2 with $x > 0.4$, R_{EMC}^d tends to be higher than for Case 1. This arises in a region of significantly lower statistics on account of the higher W-cut and fewer kinematic points available for resonance averaging. Although the slope dR_{EMC}^d/dx in this case is consistent with zero, we find this result unstable to small changes in kinematics. Case 2 at high x figures into the systematic errors on our quoted R_{EMC}^d values, however.

Since the data span a large and relatively low Q^2 range starting at 1 GeV^2, one needs to worry about whether R_{EMC}^d is simply an artifact of structure function evolution. To study this we looked at the contents of each x-bin separately. Figure 1 shows that each x-bin covers a wide enough Q^2 range to study Q^2 variations within that bin. For this study each data point was converted into R_{EMC}^d as described above, and instead of averaging, all values were fit to a straight line vs. Q^2. Fitting to a constant slope yields $dR_{\mathrm{EMC}}^d/dQ^2 = 0.0037(45)$, which is consistent with no observable Q^2 variation.

Although the BONuS F_2 data were extracted assuming that the longitudinal-to-transverse cross section ratio R cancels in the neutron to deuteron ratios, the associated uncertainty is included in the published results. Some nuclear dependence to R could, however, slightly modify our EMC results [48].

IV. RESULTS

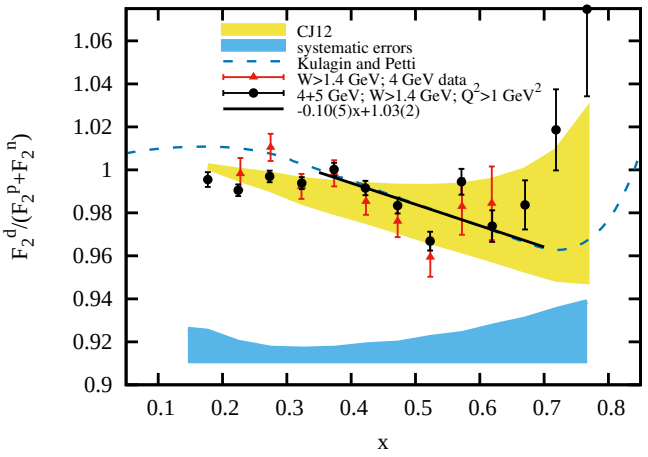

FIG. 2: (color online) The deuteron EMC ratio $R_{\mathrm{EMC}}^d = F_2^d/(F_2^n + F_2^p)$ as extracted from the BONuS data. Total systematic uncertainties are shown as a band arbitrarily positioned at 0.91 (blue). The yellow band shows the CJ12 [49] limits expected from their nuclear models. The black points are the combined 4 and 5 GeV data, whereas the red points are the 4 GeV data alone. The dashed blue line shows the calculations of Ref. [36]. The solid line (black) is the fit to the black points for $0.35 < x < 0.7$.

Our final result uses the new self-consistent convolution model [44] for F_2^p/F_2^d, which was used to determine the absolute normalization of the final published BONuS F_2^n/F_2^d data [42]. It provides an excellent representation of F_2 for our kinematics. Our result uses the combined 5.26 and 4.22 data with cuts $Q^2 > 1$ GeV^2 and $W > 1.4$ GeV. A linear fit for $0.35 < x < 0.7$ yields $dR_{\mathrm{EMC}}^d/dx = -0.10 \pm 0.05$ where the uncertainty comes from the χ^2 fit. Figure 2 shows these results together with comparisons to various models. For $x < 0.5$ the EMC ratios R_{EMC}^d agree within uncertainties with those obtained using more stringent cuts in W. The ratio for $x > 0.5$ continues the trend of the lower-x data, with a hint of the expected rise above $x = 0.7$ as seen in R_{EMC}^A for heavier nuclei, but these high-x values are more un-

certain because there are fewer data points for resonance averaging. The black circles are the combined results for 4 and 5 GeV, which are clearly dominated by the 5 GeV data. The 4 GeV data by themselves (red triangles), are consistent with the combined data set. The two points between $x = 0.5$ and 0.6 seem to be off the trend, one being high and the other low. Because this is consistent for the two beam energies, we suspect that there is a slight mismatch between the model form factors and the data in this region.

Table I gives our numerical results, in which N is the number of F_2^n/F_2^d points contributing to a bin with average kinematic values $\langle x\rangle$ and $\langle Q^2\rangle$. Here $\Delta R_{\rm EMC}^{\rm stat}$ and $\Delta R_{\rm EMC}^{\rm sys}$ are the statistical and systematic uncertainties that come from the BONuS data themselves, and $\Delta R_{\rm tot}^{\rm sys}$ is the total systematic uncertainty that includes $\Delta R_{\rm EMC}^{\rm sys}$ plus the modeling and normalization uncertainties in F_2^p/F_2^d.

TABLE I: EMC results for the deuteron. The columns correspond to the number of kinematic points, average x and Q^2, the EMC ratio, the statistical and systematic errors from the BONuS data, and the total systematic error including modeling of F_2^p/F_2^d.

N	$\langle x\rangle$	$\langle Q^2\rangle$ (GeV^2)	$R_{\rm EMC}^d$	$\Delta R_{\rm EMC}^{\rm stat}$	$\Delta R_{\rm EMC}^{\rm sys}$	$\Delta R_{\rm tot}^{\rm sys}$
28	0.177	1.09	0.995	0.003	0.002	0.015
55	0.224	1.24	0.991	0.003	0.003	0.010
65	0.273	1.39	0.997	0.003	0.003	0.007
71	0.323	1.50	0.994	0.003	0.004	0.007
70	0.373	1.63	1.000	0.003	0.005	0.007
70	0.422	1.71	0.992	0.003	0.007	0.009
71	0.472	1.85	0.983	0.004	0.009	0.009
56	0.523	2.01	0.967	0.004	0.011	0.012
47	0.572	2.30	0.994	0.006	0.013	0.014
41	0.619	2.54	0.974	0.007	0.017	0.017
26	0.670	2.97	0.984	0.011	0.020	0.021
21	0.719	3.39	1.019	0.019	0.023	0.025
11	0.767	4.03	1.075	0.041	0.024	0.029

The current results can be compared to the SLAC model-dependent extraction from Ref. [7]. Here $R_{\rm EMC}^d$ was estimated assuming the hypothesis of Ref. [50] that $1 + R_{\rm EMC}$ is proportional to the nucleon density. The SLAC slope $dR_{\rm EMC}^d/dx = -0.098 \pm 0.005$ is similar to our own, but its quoted uncertainty takes no account of the model-dependence. The assumption of density-dependence gives consistent results with our measurements for the deuteron. Semi-empirical models like that of Ref. [36] (blue dashed curve in Figure 2), which include Fermi motion, binding, and off-shell effects, are able to describe the shape of $R_{\rm EMC}^d$ quite well. Our data are also consistent with the CJ12 [49] band in yellow.

We have explored whether the Nachtmann variable $\xi = 2x/(1 + \sqrt{1 + 4M^2x^2/Q^2})$ (with M the nucleon mass) would be better suited than x to represent $R_{\rm EMC}^d$, since our data are at relatively low Q^2. The authors of Refs. [8, 47] too have addressed this question. They and we prefer x, which has been the common variable of discourse and calculation. Our EMC ratios are determined using data and model at precisely the same values of W and Q^2. Therefore, plotting versus ξ merely redistributes the EMC points along the x axis. Generally, ξ is smaller than x. Consequently, more of the high-x resonances in the data-set now contribute to the EMC slope. Thus, using ξ to reduce the effect of resonances, actually increases their influence. A fit over the rescaled interval [0.35,0.65] yields $dR_{\rm EMC}^d/d\xi = -0.08 \pm 0.06$. The slope is slightly smaller and the uncertainty slightly larger than when we plot versus x. Resonance states above $x = 0.7$ drive the slope to slightly smaller values than the fit versus x.

The analysis of Ref. [13] finds a linear relationship of the EMC slopes $dR_{\rm EMC}^A/dx$ versus the relative short-range correlation probability $R_{2N}(A/d)$ in a nucleus A with respect to the deuteron. From that analysis the authors conclude that the deuteron EMC slope should be $dR_{\rm EMC}^d/dx = -0.079 \pm 0.006$. This value is somewhat smaller than our result of -0.10 ± 0.05 but is consistent within 1σ. A more recent analysis along these same lines brackets the slope between -0.079 and -0.106 [19], and suggests that the uncertainties of Ref. [13] are underestimated.

V. $R_{\rm EMC}^d$ AND SHORT-RANGE CORRELATIONS

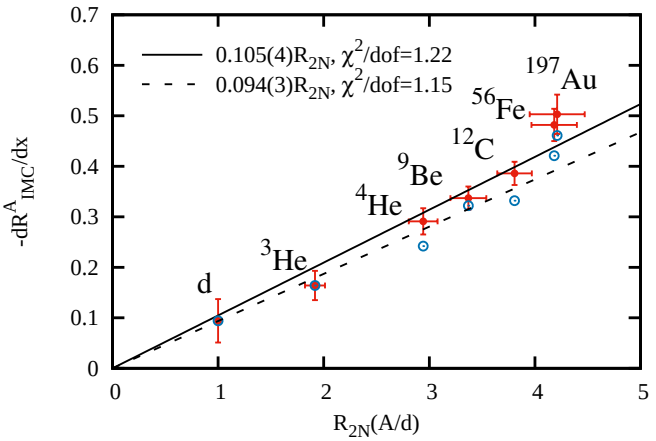

FIG. 3: (color online) EMC slopes per isoscalar nucleon, $-dR_{\rm IMC}^A/dx$, versus the relative probability with respect to the deuteron of short-range correlations, $R_{2N}(A/d)$. Fits assume that $(dR_{\rm IMC}^A/dx)/(R_{2N}(A/d))$ is constant. The red points are from Ref. [13]. The blue points are from Ref. [20] and are corrected for isospin and for x normalized to a maximum of $x = A$. Their uncertainties are the same as for the red points.

We are able to use our results to estimate the in-medium correction $R^A_{\rm IMC} = 2F_2^A/A(F_2^n + F_2^p)$ with slope $dR^A_{\rm IMC}/dx$, for which the normalizing factor is the isoscalar free nucleon. We write $R^A_{\rm EMC} = 1 + (dR^A_{\rm EMC}/dx)(x_0 - x)$ assuming that all nuclei have ratios of unity at $x_0 = 0.31 \pm 0.04$, as found in Ref. [13]. The nuclear EMC ratio $R^A_{\rm EMC}$ can be multiplied by the deuteron EMC ratio $R^d_{\rm EMC}$ to obtain $R^A_{\rm IMC}$. Hence, to good approximation, $dR^A_{\rm IMC}/dx = dR^A_{\rm EMC}/dx + dR^d_{\rm EMC}/dx$. Figure 3 shows the results. The data are consistent with the *ansatz* that $dR^A_{\rm IMC}/dx$ is directly proportional to $R_{2N}(A/d)$, the short-range correlation probability, with a proportionality constant 0.105 ± 0.004 ($\chi^2/{\rm dof} = 1.22$). This effect persists for the isospin and nuclear-x-corrected data from Ref. [20] (blue points), which have the same uncertainties as the red points. The linear relationship between short-range correlations and EMC slopes, with the shift for the deuteron EMC effect, is now consistent with an intercept of zero, and the relationship becomes a straight proportion described by a single free parameter.

VI. SYNOPSIS

In summary, we find an EMC-like slope in the ratio of deuteron to free nucleon structure functions, using the BONuS data (which are partially in the nucleon resonance region above the Δ resonance). This slope is consistent with conventional nuclear physics models that include off-shell corrections, as well as with short-range-correlation models of the EMC effect. This first, direct measurement of the magnitude of the EMC effect in deuterium demonstrates that the new BONuS experiment at 11 GeV using CLAS12, with its better precision, larger average Q^2, and deep-inelastic kinematics, will be able to determine $R^d_{\rm EMC}$ with good accuracy.

Acknowledgments

We thank the staff of the Jefferson Lab accelerator and Hall B for their support on the BONuS experiment. This work was supported by the United States Department of Energy (DOE) Contract No. DE-AC05- 06OR23177, under which Jefferson Science Associates, LLC operates Jefferson Lab. S.K., J.A., S.T., and K.G. acknowledge support from the DOE, Office of Science, Office of Nuclear Physics, under grants DE-FG02-96ER40960, DE-AC02-06CH11357, DE-FG02-97ER41025, and DE-FG02-96ER41003, respectively. I.N. and G.N. acknowledge support from the NSF under grant PHY-1307196. M.E.C. acknowledges support from NSF grants PHY-1002644 and PHY-1307415.

[1] J. Aubert et al. (European Muon Collaboration), Phys. Lett. **B123**, 275 (1983).
[2] A. Bodek, N. Giokaris, W. Atwood, D. Coward, D. Dubin, et al., Phys. Rev. Lett. **51**, 534 (1983).
[3] A. Bodek, N. Giokaris, W. Atwood, D. Coward, D. Sherden, et al., Phys. Rev. Lett. **50**, 1431 (1983).
[4] S. Dasu, P. de Barbaro, A. Bodek, H. Harada, M. Krasny, et al., Phys. Rev. Lett. **60**, 2591 (1988).
[5] J. Ashman et al. (European Muon Collaboration), Phys. Lett. **B202**, 603 (1988).
[6] P. Amaudruz et al. (New Muon Collaboration), Z. Phys. **C51**, 387 (1991).
[7] J. Gomez, R. Arnold, P. E. Bosted, C. Chang, A. Katramatou, et al., Phys. Rev. **D49**, 4348 (1994).
[8] J. Seely, A. Daniel, D. Gaskell, J. Arrington, N. Fomin, et al., Phys. Rev. Lett. **103**, 202301 (2009), 0904.4448.
[9] D. Alde, H. Baer, T. Carey, G. Garvey, A. Klein, et al., Phys. Rev. Lett. **64**, 2479 (1990).
[10] M. Arneodo, Phys. Rept. **240**, 301 (1994).
[11] D. F. Geesaman, K. Saito, and A. W. Thomas, Ann. Rev. Nucl. Part. Sci. **45**, 337 (1995).
[12] P. Norton, Rept. Prog. Phys. **66**, 1253 (2003).
[13] L. Weinstein, E. Piasetzky, D. Higinbotham, J. Gomez, O. Hen, et al., Phys. Rev. Lett. **106**, 052301 (2011), 1009.5666.
[14] L. Frankfurt, M. Strikman, D. Day, and M. Sargsian, Phys. Rev. **C48**, 2451 (1993).
[15] K. Egiyan et al. (CLAS), Phys.Rev. **C68**, 014313 (2003), nucl-ex/0301008.
[16] N. Fomin, J. Arrington, R. Asaturyan, F. Benmokhtar, W. Boeglin, et al., Phys. Rev. Lett. **108**, 092502 (2012), 1107.3583.
[17] J. Arrington, D. Higinbotham, G. Rosner, and M. Sargsian, Prog. Part. Nucl. Phys. **67**, 898 (2012), 1104.1196.
[18] O. Hen, M. Sargsian, L. Weinstein, E. Piasetzky, H. Hakobyan, et al., Science **346**, 614 (2014), 1412.0138.
[19] O. Hen, E. Piasetzky, and L. Weinstein, Phys. Rev. **C85**, 047301 (2012), 1202.3452.
[20] O. Hen, D. Higinbotham, G. Miller, E. Piasetzky, and L. Weinstein, Int. J. Mod. Phys. **E22**, 1330017 (2013), 1304.2813.
[21] C. Ciofi degli Atti, L. Frankfurt, L. Kaptari, and M. Strikman, Phys. Rev. **C76**, 055206 (2007), 0706.2937.
[22] W. Melnitchouk, M. Sargsian, and M. Strikman, Z. Phys. **A359**, 99 (1997), nucl-th/9609048.
[23] J. Arrington, A. Daniel, D. Day, N. Fomin, D. Gaskell, et al., Phys. Rev. **C86**, 065204 (2012), 1206.6343.
[24] S. A. Kulagin and R. Petti, Nucl. Phys. Proc. Suppl. **159**, 180 (2006), hep-ph/0602090.
[25] Y. Kahn, W. Melnitchouk, and S. A. Kulagin, Phys. Rev. **C79**, 035205 (2009), 0809.4308.
[26] R. Lednicky, D. Peshekhonov, and G. Smirnov, Sov. J. Nucl. Phys. **52**, 552 (1990).
[27] G. West, Phys. Lett. **B37**, 509 (1971).
[28] W. Atwood and G. B. West, Phys. Rev. **D7**, 773 (1973).
[29] L. Frankfurt and M. Strikman, Phys. Lett. **B76**, 333 (1978).
[30] D. Kusno and M. J. Moravcsik, Nucl. Phys. **B184**, 283 (1981).

[31] L. Kaptar and A. Y. Umnikov, Phys. Lett. **B259**, 155 (1991).
[32] K. Nakano and S. Wong, Nucl. Phys. **A530**, 555 (1991).
[33] W. Melnitchouk, A. W. Schreiber, and A. W. Thomas, Phys. Lett. **B335**, 11 (1994), nucl-th/9407007.
[34] M. Braun and M. Tokarev, Phys. Lett. **B320**, 381 (1994).
[35] V. Burov and A. Molochkov, Nucl. Phys. **A637**, 31 (1998).
[36] S. A. Kulagin and R. Petti, Nucl. Phys. **A765**, 126 (2006), hep-ph/0412425.
[37] J. Arrington, J. Rubin, and W. Melnitchouk, Phys. Rev. Lett. **108**, 252001 (2012), 1110.3362.
[38] J. Arrington, F. Coester, R. Holt, and T.-S. Lee, J. Phys. **G36**, 025005 (2009), 0805.3116.
[39] W. Melnitchouk and A. W. Thomas, Phys. Lett. **B377**, 11 (1996), nucl-th/9602038.
[40] H. C. Fenker, V. Burkert, R. Ent, N. Baillie, J. Evans, et al., Nucl. Instrum. Meth. **A592**, 273 (2008).
[41] N. Baillie et al. (CLAS Collaboration), Phys. Rev. Lett. **108**, 199902 (2012), 1110.2770.
[42] S. Tkachenko et al. (CLAS Collaboration), Phys. Rev. **C89**, 045206 (2014), 1402.2477.
[43] A. Accardi, W. Melnitchouk, J. Owens, M. E. Christy, C. Keppel, et al., Phys. Rev. **D84**, 014008 (2011), 1102.3686.
[44] N. Kalantarians, M. E. Christy, J. Ethier, and W. Melnitchouk, private communication, publication in preparation (2015).
[45] M. E. Christy and P. E. Bosted, Phys. Rev. **C81**, 055213 (2010), 0712.3731.
[46] P. Bosted and M. E. Christy, Phys. Rev. **C77**, 065206 (2008), 0711.0159.
[47] J. Arrington, R. Ent, C. Keppel, J. Mammei, and I. Niculescu, Phys. Rev. **C73**, 035205 (2006), nucl-ex/0307012.
[48] V. Guzey, L. Zhu, C. E. Keppel, M. E. Christy, D. Gaskell, et al., Phys. Rev. **C86**, 045201 (2012), 1207.0131.
[49] J. Owens, A. Accardi, and W. Melnitchouk, Phys. Rev. **D87**, 094012 (2013), 1212.1702.
[50] L. Frankfurt and M. Strikman, Phys. Rept. **160**, 235 (1988).